Silver nanoparticle arrays on track etch membrane support as flow-through optical sensors for water quality control

Accepted for publication in the Environmental Nanotechnology special issue of

Environmental Engineering Science journal on June 23, 2006

Final publication is available from Mary Ann Liebert, Inc., publishers

http://dx.doi.org/10.1089/ees.2007.24.122

Julian S. Taurozzi[1], and Volodymyr V. Tarabara[2,†]

[1] Department of Civil and Environmental Engineering, Michigan State University, East Lansing, MI 48824, USA.

Phone: (517) 353-9059; Fax: (517) 355-0250; Email: taurozzi@msu.edu

[2] Department of Civil and Environmental Engineering, Michigan State University, East Lansing, MI 48824, USA.

Phone: (517) 432-1755; Fax: (517) 355-0250; Email: tarabara@msu.edu

Key Words: surface-enhanced Raman scattering, silver nanoparticles, membrane-based sensors, track etch membranes, water quality

[†] Corresponding author

Abstract

Silver nanoparticle arrays were assembled on the surface of polycarbonate track etch membranes using 3-aminopropyltrimethoxysilane as the chemical linker. The assembled arrays were sub-monolayer and reproducibly regular. The nanoparticle-modified membranes were characterized in terms of their hydraulic and optical properties and were evaluated as flow-through surface-enhanced Raman scattering (SERS) sensors for water quality monitoring. The membrane-supported nanoparticle arrays were found to be SERS-active with slightly lower but significantly more reproducible enhancements in comparison with enhancements afforded by source nanoparticle suspensions. Large enhancements of up to 10^5 were demonstrated due to preconcentration by recirculating analyte solution through nanoparticle-modified membranes that were shown to retain their hydraulic properties. The findings point to the promise of combining high specification SERS-active systems and the flow-through design for the development of analytical sensors for the trace detection of aqueous pollutants.

Key Words: surface-enhanced Raman scattering, silver nanoparticles, membrane-based sensors, track etch membranes, water quality

Introduction

Timely detection of water supply contamination, accurate assessment of related risks, and development of appropriate remediation strategies depend on the availability of reliable water quality monitoring technologies (Bartram and Ballance, 1996). At the core of these technologies are deployable environmental sensors subject to such criteria as fingerprinting capability, low fouling characteristics, reproducibility, and low detection limits. The lack of sensing devices that meet these demands is the main limitation of pollution detection methods in use today.

The detection process can be viewed as consisting of two consecutive stages: (1) selective *preconcentration*/separation of pollutants and (2) *measurement* of pollutant concentration. To reliably determine the occurrence of molecular contaminants or microbial pathogens in natural and treated waters, large volumes (up to 1000 liters) of source water have to be sampled and preconcentrated to much smaller volumes. For rapid assaying of microbial pathogens, for example, acceptable concentrate volumes are smaller than 1 liter and often are as small as several milliliters (Sobsey, 1999; Hashsham, et al., 2004). In addition to separating pollutants from the system matrix, preconcentration enhances detection sensitivity, which is especially important for the detection of water pollutants in very low concentrations. The practical worth of preconcentration is exemplified by the use of membranes for the detection of microbial pathogens in aqueous systems (Juliano and Sobsey, 1997; Sobsey, 1999; Wiesner and

Chellam, 1999; Quintero-Betancourt, et al., 2002; Morales-Morales, et al., 2003; Straub and Chandler, 2003).

At the measurement stage, the employed detection methods have to be sensitive and selective. The remarkable sensitivity and molecular specificity afforded by surface enhanced Raman scattering (SERS) (Albrecht and Creighton, 1977; Jeanmaire and Vanduyne, 1977; Chang and Furtak, 1982; Moscovits, 1985; Campion and Kambhampati, 1998) makes this spectroscopic technique especially attractive for those sensing applications, where both low detection limits and fingerprinting capability are needed (Vo-Dinh, 1995). Reports of single-molecule detection using SERS (Kneipp, et al., 1996) and the design of flow-through SERS systems (Weissenbacher, et al., 1998) have further amplified interest in possible uses of this technique for environmental sensing (Mullen, et al., 1992; Weissenbacher, et al., 1997; Vo-Dinh, 1998; Sanchez-Cortes, et al., 2001; Mosier-Boss and Lieberman, 2003).

The SERS effect can be observed when a light-scattering molecule is adsorbed on a SERS-active substrate, typically a roughened surface of certain coinage metals, gold and silver being primary examples. The choice of the type of the enhancing substrate remains application-specific because different types of SERS-active substrates exhibit different properties; island metal films on a solid support, for example, are more stable, while for aggregated metal colloids higher enhancements are generally expected (Kneipp, et al., 1998). What all SERS-active systems have in common, however, is that the morphology

of substrates has a profound effect on their optical properties. In the case of nanoparticle suspensions, the relatively poor stability of sols and the dependence of nanoparticle aggregate morphology on the nature and concentration of the analyte partly offsets the advantage of high enhancements typical of such substrates. The difficulty in fabricating SERS-active substrates that reproducibly yield high enhancements is the single most significant factor that hampers further applications of the SERS method for sensing. Development of highly enhancing, but also stable, reproducible, and robust SERS-active substrates is, therefore, very important for SERS to mature into an "off-the-shelf" detection method.

One approach to improve reproducibility of SERS is the immobilization of nanoparticles on stable supports (e.g. Luo and Fang, 2005; Volkan, et al., 2005). Permeable supports are of particular interest as they may allow for the added advantage of preconcentration. The idea of using filters as SERS substrates has been approached previously from different perspectives by several research groups (Laserna, et al., 1988; Kurokawa and Imai, 1991; Lee and Li, 1994; Walsh and Chumanov, 2001; Muniz-Miranda and Innocenti, 2004). The studies involved coverage of a permeable substrate - filter paper or aluminum based membranes - with silver nanoparticles. The substrate preparation has been based either on the filtration of silver colloids through polymeric membranes (Muniz-Miranda and Innocenti, 2004) or on the chemical reduction of silver directly on the filter surface (Laserna, et al., 1988; Lee and Li, 1994). Since the filtration-based methods involved retention of silver particles in the membranes, the filtering ability of

such membranes could be expected to be greatly inhibited. Recently, the method of vacuum deposition of silver onto an aluminum membrane filter was reported wherein the filter permeability could be expected to remain unchanged (Walsh and Chumanov, 2001). By filtering a small amount of analyte solution through the membrane, an improved detection capability was demonstrated.

The objective of this work was to develop flow-through SERS-active substrates by assembling arrays of silver nanoparticles on the surface of track etch polycarbonate membranes (Apel, 2001; Han, et al., 2005). Previously, nitrogen functionalities have been successfully introduced to polycarbonate and other polymeric structures by using plasma treatment (Jama, et al., 1996; Gancarz, et al., 2000; Schroder, et al., 2001; Bryjak, et al., 2002; Kull, et al., 2005) and by employing the reactivity of polycarbonate with amines (Foldi and Campbell, 1962; Ishida and Lee, 2002). Our approach was to employ 3-aminopropyltrimethoxysilane and cysteamine as chemical linkers between polycarbonate surface and silver nanoparticles. SERS enhancing properties of resulting membrane-supported arrays were tested and compared with those of source nanoparticle suspensions using methylene blue (MB) as an analyte relevant for pathogen detection and inactivation techniques (e.g. Murinda, et al., 2002; Pelletier, et al., 2006). Finally, we considered sensitivity in a broader context that included membrane-enabled preconcentration as the factor that augments the inherently high sensitivity of nanoparticle-based SERS substrates and studied the effect of preconcentration on the sensitivity of the developed sensors.

Materials and Methods

The ultrapure water used in the experiments was supplied by a commercial ultrapure water system (Lab Five, USFilter Corp., Hazel Park, MI) equipped with a terminal 0.2 μm capsule microfilter (PolyCap, Whatman Plc., Sanford, ME). The resistivity of water was greater than 16 MΩ·cm. Boil off nitrogen and 99.9999 % purity argon gases were used in the plasma experiments.

Synthesis of silver nanoparticles

Aqueous suspensions of silver nanoparticles (Ag hydrosols) were prepared using the procedure described by Lee and Meisel (Lee and Meisel, 1982). 90 mg of silver nitrate were added to 500 mL of ultrapure water and brought to 100 ^{0}C. 10 mL of 1 % by weight solution of trisodium citrate were added dropwise to the boiling water under vigorous stirring. To prepare sols with a narrower particle size distribution, sodium citrate solution was added as quickly as possible and in the smallest droplets possible. Gradual color change of the solution from transparent to greenish gray was indicative of the progress of silver particle nucleation reaction. The erlenmeyer flask containing the solution was loosely capped with a ceramic crucible to avoid significant solvent loss due to evaporation. After 40 minutes of boiling, the hydrosol was left to cool down. The loss of water to evaporation was compensated by the addition of ultrapure water to restore the

original volume of 500 mL. After allowing the hydrosol to cool down to room temperature, it was stored at 4 ^{0}C.

To precoagulate sol, 100 μL of silver sol were mixed with 100 μL of ultrapure water and 10 μl of a 0.5 mol/L $NaClO_4$ aqueous solution. For SERS measurements in precoagulated Ag hydrosols, 30 μL of the precoagulated suspension were removed and 20 μL of the analyte solution were added, yielding a final 1:10 dilution of the sample in the precoagulated sol. The resulting preparation was used for SERS measurements.

Membranes and membrane surface modification

25 mm diameter, 5 μm nominal pore size hydrophobic polyvinylpyrrolidone(PVP)-free polycarbonate track etch (PCTE) membrane filters were purchased from Sterlitech (Sterlitech Corp, Kent, WA). Based on the value of pore density ($4 \cdot 10^5$ pores/cm^2) reported by the manufacture the average distance between pores was estimated to be ca. 16 μm.

Two approaches to membrane modification were explored. The first approach was to treat membranes with nitrogen plasma to directly introduce nitrogen functionalities on the membrane surface, or to treat membranes with argon plasma and then immerse them in allylamine to introduce reactive radicals on the polycarbonate surface that would later react with the unsaturated bond of allylamines. The second approach was the direct interfacial reaction of polycarbonate with amine containing molecules, APTMS or CysA.

Nitrogen plasma and argon/allylamine plasma treatment. Bare (non-modified) membranes were subjected to pure nitrogen plasma treatment. A plasma etching system (PX-250, March Instruments, Concord, CA), connected to a pure nitrogen supply at 9 scfm constant flow was used to generate the plasma. After 5 minutes of plasma treatment, membranes were immersed in silver hydrosol for 24 hours. In a separate set of experiments, bare membranes were subjected to pure argon plasma treatment using the plasma etching system and flow rate described above. After 5 minutes of plasma treatment, membranes were immersed in a 1 % by weight allylamine aqueous solution for 5 minutes, rinsed with ultrapure water for 1 hour and immersed in silver hydrosol for 24 hours. After each treatment, membranes were separated from the silver sol and rinsed with ultrapure water to eliminate excess hydrosol. The modified membranes were kept in ultrapure water until further use.

APTMS used as a linker. It has been shown that closely packed arrays of gold and silver particles can be assembled on a surface of a glass slide modified with APTMS (Grabar, et al., 1995). Other studies have shown that aminosilanes react with polycarbonate via the amino group (Wilkes and Li, 1997); the proposed reaction pathway for the APTMS/polycarbonate reaction can be seen in Fig. 1. The membranes were immersed in a 25 % by weight solution of APTMS in methanol for 5 minutes. After incubation in APTMS, membranes were rinsed in pure methanol for 45 minutes with three changes of the solvent. After the final rinse, membranes were immersed in silver hydrosol for 24 hours. Aggregation of silver suspension in the immediate vicinity of the derivatized membrane initiated by residual physisorbed APTMS was indicative of poor rinsing and

such samples were discarded. The aggregation could be recognized by an initial darkening of the suspension, a gradual increase in transparency, and appearance of a lilac tint in the suspension. Prolonged rinsing in methanol was found to be necessary to avoid these effects.

CysA used as a linker. In the case of CysA, the amino group would preferentially react with the polycarbonate surface leaving an available thiol group for silver chemisorption. The membranes were immersed in a 3.24 mol/L aqueous solution of CysA for 60 minutes. After CysA incubation, membranes were rinsed in ultrapure water for 15 minutes with three changes of the solvent. After the final rinse, membranes were immersed in silver hydrosol for 24 hours.

XPS, UV-vis, Raman and SERS measurements

XPS measurements of bare and APTMS-modified membranes were conducted using PHI 5400 ESCA system (Physical Electronics, Chanhassen, MN), equipped with a non-monochromatic Mg X-Ray. Measurements were done using a take off angle of 45 degrees. Raman and SERS spectra were recorded at a spectral resolution of 5 cm^{-1} and coverage from 250 cm^{-1} to 4,000 cm^{-1} using Kaiser Optical Systems HoloProbe Raman spectrograph coupled to an Olympus BX-60 optical microscope and equipped with a motorized sample stage. A frequency doubled YAG laser emitting at 532 nm with a beam power of 5 mW was employed as the excitation source. The laser spot diameter was less than 2 μm (with 100x objective). Exposure times (5 ms to 5 s) and the number of

accumulations (1 to 25) were adjusted in each measurement to avoid detector saturation. Measured intensity values were normalized to account for variations in exposure times and accumulations. To record Raman signal from membrane-based substrates, the substrates were placed on the sample stage with the SERS-active surface facing the microscope lens. To record Raman signal from liquid samples and hydrosols, the samples were transferred to glass capillaries with ca. 2 mm internal diameter; the laser beam was then focused on the center of the capillary containing the sample.

UV-vis absorption spectra of the silver hydrosol and treated membranes were recorded using a photodiode array spectrophotometer (Multi-Spec 1501, Shimadzu, Kyoto, Japan). Spectral coverage was from 180 nm to 800 nm with a spectral sampling interval of 1 nm and with 100 accumulations per measurement. Absorption spectra of ultrapure water and bare membranes were used as baselines in measurements of absorption of hydrosols and treated membranes, correspondingly. Measurements were performed using square quartz cells of 3 mL nominal capacity (Fisherbrand quartz, Fisher Scientific International, Hampton, NH).

Particle size and zeta potential measurements

Particle size distribution of the prepared silver hydrosol was measured using multi-angle light scattering apparatus (ZetaPALS, BI_MAS Option, Brookhaven Instrument Corp., Holtsville, NY) equipped with a solid state laser emitting 15 mW beam at 660 nm. Measurements were recorded in 10 cycles of 2 minutes each, with a 30 % cutoff dust

filter, using 3 mL sample cells provided by the equipment manufacturer. Samples were diluted in a 10 mmol/L KCl solution to reach a measurement count rate in the range of 50 kcps to 500 kcps. Zeta potential was measured by phase analysis light scattering (ZetaPALS, Brookhaven Instrument Corp., Holtsville, NY) using the same laser line as the particle sizing module described above. Measurements were conducted in 10 runs of 10 cycles each, using 3 mL sample cells provided by the equipment manufacturer. Samples were diluted in a 1 mmol/L KCl solution prior to measurements.

SEM and TEM imaging

SEM imaging was carried out using Hitachi S-4700II Field Emission scanning electron microscope operated in high vacuum, ultra high resolution mode. Samples were mounted on aluminum SEM specimen stubs, membrane sample surfaces were made conductive by sputtering gold on them for 3 minutes at a current of 20 mA (Emscope SC 500 sputter coater) prior to the SEM imaging. For higher resolution, smaller electron beam spot size and shorter working distances were employed. Samples were also imaged by transmission electron microscopy (JEOL JEM 2010, JEOL USA, Inc., Peabody, MA). Copper (cat. no. 3HGC500, Electron Microscopy Sciences, Hatfield, PA) and formvar carbon covered copper (cat. no. 200-CU) TEM grids were used to support the samples. The grids were drop-coated by Ag hydrosol and examined at an accelerating voltage of 100 kV.

SERS characterization of APTMS modified membranes

To assess the Raman enhancing properties of membrane-based substrates, methylene blue (MB) was used as a test compound. Aqueous solutions of MB with concentrations ranging from 10^{-4} mol/L to 10^{-7} mol/L were tested on the modified membranes. 20 μL of each solution were dropped on the surface of a modified membrane and let to dry ("drop and dry" method). For each concentration, measurements were conducted on five different membranes, on three different areas of each membrane's surface.

Membranes filtration performance

Clean water flux tests were conducted to determine intrinsic membrane resistance. Amicon 8010 ultrafiltration cell (Millipore Corp, Billerica, MA) was used as the membrane module. Variable feed water flow rate was achieved by varying the delivery pressure of the compressed zero air tank. Ultrapure water was stored in a pressurized container (100 psi, 5L, Alloy Products Corp., Waukesha, WI). Pressurized air from the air tank pressure regulator (cat no. 8069621, Controls Corp. of America, VA. Beach, VA) connected to the inlet of the water container was used to deliver feed water to the filtration cell. The permeate flux was measured continuously by collecting the filtered water on a digital weighing balance (AV8101C, Ohaus Corp., Pine Brook, NJ) interfaced with a computer via a built-in RS-232 port. In all experiments, the feed water flow rate was sequentially increased by increasing the outlet pressure of the compressed zero air tank from 0 psi to 28 psi. The data from the weighing balance was logged to a computer using a program written in LabView (version 7.1, National Instruments). Data were

acquired at a 5 s time interval. Clean water flux tests were conducted both for untreated membranes and modified membranes.

Preconcentration studies

A variable flow rate positive displacement pump (model XX80EL000, Millipore Corp, Billerica, MA) was used to deliver feed aqueous solution of MB into the filtration cell (Amicon 8010, Millipore Corp, Billerica, MA) containing the modified membrane. The permeate flux was directed back into the feed solution container to allow for continuous recirculation of the solution. Dilute solutions of the tested compound were recirculated through the APTMS modified membranes for 2 hours. To evaluate the effect of flow-induced preconcentration, a modified membrane was immersed for 2 hours in a solution of equal concentration to that used for the preconcentration experiments, and then let to dry.

Results and Discussion

Silver nanoparticle hydrosol

Prepared hydrosols had suspended solids fraction of $3 \cdot 10^{-4}$ by weight and ionic strength of ca. $8.6 \cdot 10^{-3}$ mol/L, as calculated based on the amount of citrate and nitrate salts used in the preparation of the hydrosol. No aggregation was observed in the stored hydrosols over the duration of experiments. Figure 2 shows SEM and TEM micrographs of the

silver nanoparticles. Two types of particles were observed – ones that were approximately spherical and ones that were rod shaped, the former type being clearly predominant.

Effective diameter of silver nanoparticles in the hydrosol, as measured using light scattering, was found to be 58.8 nm ± 0.6 nm with a polydispersivity factor (Brown, et al., 1975) of 0.319 ± 0.004. As Fig. 3 illustrates, particle size distribution profile of the sol shows two major peaks at 13.76 nm and 78.86 nm and two minor peaks with effective diameters higher than 500 nm. The first two peaks can be attributed to spherical particles. The peaks that correspond to larger particles together with the relatively high polydispersivity of the measurement are likely to be due to the presence of rod-shaped particles that skew the size distribution pattern to higher diameters. To estimate the length of rod shaped particles, the following expression for the diffusion coefficient of rod-shaped particles can be used (Mishra, et al., 2000):

$$D = k_B T \frac{6 - 0.5(\gamma_{\parallel} + \gamma_{\perp})}{3\pi\eta_0 L}, \qquad (1)$$

where

$$\gamma_{\parallel} = 1.27 - 7.4\left(\delta^{-1} - 0.34\right)^2,\ \gamma_{\perp} = 0.19 - 4.2\left(\delta^{-1} - 0.39\right)^2,\ \delta = \ln\left(\frac{2L}{w}\right)$$

and D is the particle diffusion coefficient; k_B is the Boltzmann constant, T is the absolute temperature, η_0 is the viscosity of the suspending liquid, L is the rod length, and w is the rod width. By comparing equation (1) and the expression for the diffusion coefficient of

spherical particles, $D = \frac{k_B T}{3\pi\eta_0 d}$ (2), a relationship between sphere diameter and rod length for an equal diffusion coefficient can be obtained:

$$L = d[6 - 0.5(\gamma_{\parallel} + \gamma_{\perp})]. \quad (3)$$

Using the above analysis, the equivalent rod lengths were calculated to be ca. 2.9 μm and 3.5 μm.

Zeta potential of the silver sol, calculated using the Smoluchowski model, was found to be -24.27 mV ± 0.98 mV, which was indicative of a stable suspension.

Modified membranes characterization

Surface chemistry

To evaluate surface chemistry of membranes derivatized with APTMS, XPS studies were conducted. Prior to treatment, XPS analysis showed the presence of carbon and oxygen with peaks C(1s)[0.314] = 84.14 % and O(1s)[0.733] = 15.86 %, in accordance with the chemical composition of a bare polycarbonate surface. After APTMS treatment, nitrogen and silica peaks appeared as follows, C(1s)[0.314] = 77.70 %, N(1s)[0.499] = 1.80 %, O(1s) [0.733] = 18.75 % and Si(2p)[0.368] = 1.75 % indicating the presence of APTMS at the membrane surface.

Silver nanoparticle array morphology

Under the hydraulic conditions tested in our experiments, particles were not removed from the membrane surface. However, under mechanical stress, such as tapping or scratching, the particles could be easily removed; the modified membranes, therefore, were handled using tweezers and were stored immersed in ultrapure water in a Petri dish.

The distribution of nanoparticles on the membrane surface was evaluated using SEM imaging. Figure 4A illustrates the flat surface and narrow pore size distribution of a bare PCTE membrane. Figure 4 (B, D) shows the membrane surface after modification by APTMS and silver. Homogeneous sub-monolayer coverage of the membrane surface by silver nanoparticles, as well as some internal pore coverage can be observed. The membrane surface coverage by silver particles was determined using image processing (ImageJ v1.34s, National Institutes of Health, USA) of SEM micrographs of modified membranes (Figures 4B, 4D). The surface coverage was calculated to be 56.6%. Figure 4 (E, F) shows silver nanoparticle coverage of a CysA-modified membrane; in this case surface aggregation is evident and the coverage is less homogeneous in comparison with that of membranes modified using APTMS as a linker. Interestingly, those membranes modified using CysA as a linker did not show Raman enhancement properties while membranes modified using APTMS as a linker were SERS-active. This could be attributed to the possibility of chemisorption of remnant cysteamine molecules onto the silver nanoparticles during the silver immersion stage of membrane modification. This would hamper direct analyte-silver nanoparticle interaction and weaken SERS signal. Plasma treatments with subsequent incubation of treated membranes in the silver

hydrosol did not result in any noticeable coverage of the membranes surface by silver particles.

Optical properties of modified membranes

Optical properties of nanoparticle arrays were studied with UV-vis absorption and Raman spectroscopy. UV-vis analysis of the modified membranes was possible due to the semi-translucent nature of the membranes. In the absorption spectrum of the Ag hydrosol, a broad band at 410 nm is observed, which corresponds to the surface plasmon resonance within primary particles. The same band, but blue shifted by (13.2 ± 1.5) nm (95 % confidence) with respect to the silver sol absorption peak was observed for the silver nanoparticles attached to the modified membranes (Fig. 5). The shift was attributed to preferential exclusion of larger particles, including rod-shaped particles, from the membrane surface, as indicated by SEM results. The fact that a band at larger wavelengths does not emerge in the absorption spectrum of the modified membrane points to the absence of electromagnetic coupling between primary particles that is at the absence of surface aggregation. This observation is corroborated by SEM imaging results.

To evaluate Raman enhancing properties of modified membranes and compare them with those of source hydrosols, MB was chosen as the test compound. Figure 6 shows UV and Raman spectra of MB with relevant band assignments (Naujok, et al., 1993), as well as the chemical structure of this compound. The excitation wavelength used in this work

was 532 nm that is far from the resonance frequency of MB. Much lower detection limits, and perhaps higher enhancements factors, could have been observed had the resonant excitation been chosen. Nonetheless, this laser line is suitable for the comparison of modified membranes and silver hydrosol with respect to their Raman enhancing properties, which was one of the goals of this study.

First, Raman spectra of bare and modified membranes were recorded. In contrast to the spectrum of the bare membrane, the spectrum of the modified membrane was found to be relatively featureless (Fig. 7). Raman spectra of aqueous solutions of MB with concentrations ranging from 10^{-7} mol/L to 10^{-2} mol/L were then measured. The two most intense peaks on the Raman spectrum, 1401 cm^{-1} and 1626 cm^{-1}, correspond to the symmetric CN stretch and CC ring stretch, respectively. A linear increase in Raman intensity for both these peaks was observed for solutions in the 10^{-5} mol/L to 10^{-3} mol/L range. To avoid saturation effects, Raman intensity recorded for 10^{-4} mol/L solutions was used in the computation of enhancement SERS enhancement factors.

To evaluate the Raman enhancement of assembled nanoparticle arrays, Raman spectra from solutions of known concentrations of MB on the membrane surface were recorded and compared to those obtained from the same solution concentrations on the precoagulated silver hydrosol. Figure 8 shows the Raman spectra recorded for a 1 mmol/L solution of MB, and the enhanced peaks from silver sol and modified membrane at 1626 cm^{-1}. A slight shift of the peaks can be observed, pointing to varying MB/silver nanoparticles interactions for the different enhancing substrates. To calculate the

enhancement factors of the silver sol and the modified membranes, the following equation was used:

$$EF = \frac{I_a C_b}{I_b C_a}, \quad (4)$$

where I_a and I_b indicate the normalized Raman intensities for a given peak, I_a being the enhanced intensity (from the Ag hydrosol or the modified membranes) and I_b the comparative basis, at MB concentrations C_a and C_b. By comparing intensities of the 1626 cm^{-1} peak in the SERS spectrum of a) 0.01 mmol/L solution of MB at the modified membrane surface and b) 10^{-6} mol/L solution of MB enhanced by precoagulated sol with Raman signal from 10^{-4} mol/L aqueous MB solution, average enhancement factors of 157.9 (t95%=141.3) and 111.7 (t95%=11.8) were obtained for silver sol and modified membrane, respectively, considering all possible intensity combinations between enhanced peaks and source MB peaks. While the EF of the sol is slightly higher than that of the modified membrane, so is the standardized error, indicating that the modified membranes have better SERS reproducibility than the sols. The observed EF values are summarized in the Fig. 9. The main body (box) of the plot encloses the middle 50% range of the EF measurements (and excludes lower and upper quartiles of the data set) while the line that crosses the box corresponds to the EF data median. Whiskers indicate the sample maximum and minimum, and open circles correspond to outliers. As can be seen from Fig. 9, the spread in EF values significantly higher for the precoagulated sol than for sols, indicative of lower reproducibility. A narrower and more symmetric distribution can be observed for the modified membranes; also, the median value of EF from modified membranes was higher than that for the hydrosol.

Filtration performance of modified membranes

To study possible changes in the filtration performance of membranes after modification, clean water flux tests were conducted both for untreated membranes and nanoparticle-modified membranes (Fig. 10). Membrane resistance was calculated to be ($1.09 \cdot 10^7 \pm 0.01$) m^{-1} and ($1.15 \cdot 10^7 \pm 0.02$) m^{-1} for bare and modified membranes, respectively. As Fig. 10 illustrates, the flux versus pressure trendline was drawn for the first three points only, using linear least square fitting. The subsequent points were not considered since they did not follow the linear trend, likely due to membrane pore constriction at higher transmembrane pressure differentials. The above measurements clearly indicate that the particle attachment to membrane surface did not result in any significant changes in the membrane resistance.

Preconcentration

We considered sensitivity in a broader context that included membrane-enabled preconcentration as the factor that augments the inherently high sensitivity of nanoparticle-based SERS substrates. To evaluate the effect of preconcentration on the sensitivity of the developed sensors, an aqueous solution of known concentration (10^{-7} mol/L) of MB was filtered through the membrane at a constant volume flow of 4 mL/sec for 2 hours. The membrane was let to dry and the SERS spectrum of MB at the membrane surface was then recorded. To ensure that any increased enhancement was solely due to preconcentration, parallel measurements were conducted both for modified

membranes immersed in a 10^{-7} mol/L MB(aq) solution for 2 hours, and modified membranes inoculated with a 10^{-7} mol/L MB (aq) solution using “drop and dry” method. While no MB peaks where observed in the SERS spectrum from the modified membranes after “drop and dry” or 2 hours immersion, preconcentration resulted in the appearance of the 1390 cm^{-1} peak (Fig. 11). For all tested membranes, the preconcentration experiments have reproducibly resulted in an improved detection limit. Interestingly, the MB peak at 1627 cm^{-1} did not appear after preconcentration, instead, the 1401 cm^{-1} peak was shifted 10 cm^{-1} with respect to its original position. Shifts could also be noticed at the precoagulated sol and modified membranes; the shifts in SERS are indicative of the disturbance of the electronic configuration of an analyte due to chemisorption. We attribute the difference in SERS spectra form MB chemisorbed by the “drop and dry” method and chemisorbed during preconcentration experiments to the different molecule-surface interactions. Convective forces present during preconcentration together with the natural hydrophobicity of the membrane substrates might favor MB chemisorption to the silver nanoparticles through the CN bond, rather than through the less polar CC bond, which could explain the predominance of the CN peak.

Based on the intensity of the 1401 cm^{-1} band in the Raman spectrum of a 10^{-2} mol/L MB aqueous solution, the enhancement factor (EF) was calculated using (4) to be $1.17 \cdot 10^{5}$ ($t95\% = 1.92 \cdot 10^{4}$); the data distribution can be observed in Figure 9B. This result shows that preconcentration is effective in increasing the enhancement provided by the membrane substrate and that the detection limit can be significantly lowered (since by

"drop and dry" or prolonged immersion no detection of MB 10^{-7} mol/L was possible). Additionally, the spread in the measurements (with respect to the EF value) is one order of magnitude lower than the averaged EF; for precoagulated silver sols the the relative width of the spread is considerably larger.

The effect of convective flow across the membrane on the improved MB adsorption to nanoparticles immobilized on the membrane surface can be rationalized in terms of diffusive and convective transport of analyte molecules. The thickness of the boundary layer formed by a fluid in motion in the vicinity of a flat plate can be roughly estimated as (Schlichting, 1968):

$$\delta = \sqrt{\frac{\nu l}{u}}, \tag{5}$$

where δ is the boundary layer thickness, ν is the kinematic viscosity of the fluid, l is the plate length, and u is the velocity of the fluid far from the surface. In our experiments, $u = j / A$, where j is the volumetric flowrate and A is the membrane area. Given that u $=0.8 \cdot 10^{-4}$ m/s and taking l to be the average distance between pores (ca. 16 μm), the thickness of the boundary layer can be estimated from (5) to be ca. 45 μm. The time it takes for a molecule to be transported by Brownian diffusion across the boundary layer is then given by:

$$t_d = \frac{\langle \delta \rangle^2}{2D}, \tag{6}$$

where D is the diffusion coefficient of the solute. By estimating the molar volume of MB by the LeBas method (LeBas, 1915) and using Hayduk-Laudie correlation (Hayduk and

Laudie, 1974) applicable to small (MW<1000 Da) non-electrolyte solutes to estimate the diffusion coefficient of MB, we obtain $D \approx 2.96 \cdot 10^{-10}$ m^2/s. Now, using (6) t_d is estimated to be ca 3.4 ms, which is of the same order of magnitude as time $t_c \approx l/u$ =2 ms that the analyte molecule spends in the vicinity of the membrane. This means that by imposing the convective flow, the boundary layer is compressed sufficiently in our experiments, for the MB molecules to be able to diffuse across the boundary layer to the upstream membrane surface as they are transported by the convective flow past the membrane surface and into the membrane pore.

This balance between convective and diffusive transport can also be viewed in terms of the probability of a solute molecule to reach (and chemisorb to) the silver coated membrane surface. Equation (6) can be rewritten as:

$$u_d = \frac{2D}{d}, \tag{7}$$

where u_d can be interpreted as the velocity of a solute that travels a distance d due to Brownian motion. A "pseudo" Peclet number can be obtained as the ratio of convective to diffusive velocities:

$$\frac{u}{u_d} = \frac{ud}{2D} \tag{8}$$

As can be seen from equation (8), this ratio will be directly proportional to the convective velocity and the distance from the membrane surface. For a fixed u, for all distances $d > \frac{2D}{u}$ the ratio (8) will be higher than one, implying that more molecules will be driven to the membrane per unit time when convection is present, than when only

diffusion occurs, thereby enhancing mass transport of the analyte to the membrane surface.

Conclusions

Silver nanoparticle arrays were assembled on track etch membrane supports and established to be SERS-active with reproducible Raman enhancements. The improved reproducibility was attributed to the well defined geometry of track etch membranes. The hydrodynamic control of analyte transport to the permeable SERS-active surface was demonstrated to allow for a dramatic improvement of the detection limit of the sensor. Better insight into processes that govern analyte partitioning from dissolved phase onto the surface of the permeable substrate is needed; boundary layer structure, membrane morphology, and surface chemistry of membrane and SERS-active sites are likely to determine the extent of preconcentration. The reported findings indicate the potential benefit of combining high specification SERS-active systems and the flow-through design for the development of analytical sensors for the trace detection of pollutants in water.

Acknowledgements

This material is based upon work supported by the National Science Foundation under Grant No. OISE-0530174. Authors thank Eliza Tsui (Rice University) for recording TEM

images of silver hydrosol particles and Dr. Jérôme Rose (Centre Européen de Recherche et d'Enseignement des Géosciences de l'Environnement) for assisting with high resolution SEM imaging of filtered Ag hydrosol particles. Helpful comments by two anonymous reviewers are gratefully acknowledged. Any opinions, findings, and conclusions or recommendations expressed in this material are those of the authors and do not necessarily reflect the views of the National Science Foundation.

References

1. ALBRECHT, M. G.; CREIGHTON, J. A. (1977). Anomalously intense Raman-spectra of pyridine at a silver electrode. *J. Am. Chem. Soc.* **99**, (15), 5215-5217.
2. APEL, P. (2001). Track etching technique in membrane technology. *Radiat. Meas.* **34**, (1-6), 559-566.
3. BARTRAM, J.; BALANCE, R. (1996). *Water Quality Monitoring*. Spon Press.
4. BROWN, J. C.; PUSEY, P. N.; DIETZ, R. (1975). Photon Correlation Study Of Polydisperse Samples Of Polystyrene In Cyclohexane. *Journal Of Chemical Physics* **62**, (3), 1136-1144.
5. BRYJAK, M.; GANCARZ, I.; POZNIAK, G.; TYLUS, W. (2002). Modification of polysulfone membranes 4. Ammonia plasma treatment. *Eur. Polym. J.* **38**, (4), 717-726.
6. CAMPION, A.; KAMBHAMPATI, P. (1998). Surface-enhanced Raman scattering. *Chem. Soc. Rev.* **27**, (4), 241-250.
7. CHANG, R. K.; FURTAK, T. E. (1982). *Surface Enhanced Raman Scattering*. New York:Plenum Press.
8. FOLDI, V. S.; CAMPBELL, T. W. (1962). Preparation of copoly(carbonate-urethanes) from polycarbonates. *J. Polym. Sci.* **56**, (163), 1-9.
9. GANCARZ, I.; POZNIAK, G.; BRYJAK, M. (2000). Modification of polysulfone membranes 3. Effect of nitrogen plasma. *Eur. Polym. J.* **36**, (8), 1563-1569.
10. GRABAR, K. C.; FREEMAN, R. G.; HOMMER, M. B.; NATAN, M. J. (1995). Preparation and characterization of Au colloid monolayers. *Anal. Chem.* **67**, (4), 735-743.
11. HAN, K. P.; XU, W. D.; RUIZ, A.; RUCHHOEFT, P.; CHELLAM, S. (2005). Fabrication and characterization of polymeric microfiltration membranes using aperture array lithography. *J. Membr. Sci.* **249**, (1-2), 193-206.
12. HASHSHAM, S. A.; WICK, L. M.; ROUILLARD, J. M.; GULARI, E.; TIEDJE, J. M. (2004). Potential of DNA microarrays for developing parallel detection tools

(PDTs) for microorganisms relevant to biodefense and related research needs. *Biosens. Bioelectron.* **20**, (4), 668-683.
13. HAYDUK, W.; LAUDIE, H. (1974). Prediction of diffusion-coefficients for nonelectrolytes in dilute aqueous-solutions. *AlChE J.* **20**, (3), 611-615.
14. ISHIDA, H.; LEE, Y. H. (2002). Study of exchange reaction in polycarbonate-modified polybenzoxazine via model compound. *J. Appl. Polym. Sci.* **83**, (9), 1848-1855.
15. JAMA, C.; DESSAUX, O.; GOUDMAND, P.; MUTEL, B.; GENGEMBRE, L.; DREVILLON, B.; VALLON, S.; GRIMBLOT, J. (1996). Surface modifications of polycarbonate (PC) and polyethylene terephtalate (PET) by cold remote nitrogen plasma (CRNP). *Surf. Sci.* **352**, 490-494.
16. JEANMAIRE, D. L.; VANDUYNE, R. P. (1977). Surface Raman spectroelectrochemistry.1. Heterocyclic, aromatic, and aliphatic-amines adsorbed on anodized silver electrode. *J. Electroanal. Chem.* **84**, (1), 1-20.
17. JULIANO, J.; SOBSEY, M. D. (1997).Simultaneous concentration of Cryptosporidium, bacteria and viruses from water by hollow fiber ultrafiltration. In *Proceedings of the Water quality technology Conference*, American Water Works Association: Denver, CO.
18. KNEIPP, K.; KNEIPP, H.; MANOHARAN, R.; HANLON, E. B.; ITZKAN, I.; DASARI, R. R.; FELD, M. S. (1998). Extremely large enhancement factors in surface-enhanced Raman scattering for molecules on colloidal gold clusters. *Appl. Spectrosc.* **52**, (12), 1493-1497.
19. KNEIPP, K.; WANG, Y.; KNEIPP, H.; ITZKAN, I.; DASARI, R. R.; FELD, M. S. (1996). Population pumping of excited vibrational states by spontaneous surface-enhanced Raman scattering. *Phys. Rev. Lett.* **76**, (14), 2444-2447.
20. KULL, K. R.; STEEN, M. L.; FISHER, E. R. (2005). Surface modification with nitrogen-containing plasmas to produce hydrophilic, low-fouling membranes. *J. Membr. Sci.* **246**, (2), 203-215.
21. KUROKAWA, Y.; IMAI, Y. (1991). Surface-enhanced Raman-scattering (SERS) using polymer (cellulose-acetate and Nafion) membranes impregnated with fine silver particles. *J. Membr. Sci.* **55**, (1-2), 227-233.
22. LASERNA, J. J.; CAMPIGLIA, A. D.; WINEFORDNER, J. D. (1988). Surface-enhanced Raman spectrometry on a silver-coated filter-paper substrate. *Anal. Chim. Acta* **208**, (1-2), 21-30.
23. LEBAS (1915). *The molecular volumes of liquid chemical compounds*. London.
24. LEE, A. S. L.; LI, Y. S. (1994). Surface-enhanced Raman-spectra using silver-coated paper substrates. *J. Raman Spectrosc.* **25**, (3), 209-214.
25. LEE, P. C.; MEISEL, D. (1982). Adsorption and surface-enhanced Raman of dyes on silver and gold sols. *J. Phys. Chem.* **86**, (17), 3391-3395.
26. LUO, Z. X.; FANG, Y. (2005). SERS of C-60/C-70 on gold-coated filter paper or filter film influenced by the gold thickness. *J. Colloid Interface Sci.* **283**, (2), 459-463.
27. MISHRA, S. R.; RAWAT, H. S.; MEHENDALE, S. C.; RUSTAGI, K. C.; SOOD, A. K.; BANDYOPADHYAY, R.; GOVINDARAJ, A.; RAO, C. N. R. (2000). Optical limiting in single-walled carbon nanotube suspensions. *Chem. Phys. Lett.* **317**, (3-5), 510.
28. MORALES-MORALES, H. A.; VIDAL, G.; OLSZEWSKI, J.; ROCK, C. M.; DASGUPTA, D.; OSHIMA, K. H.; SMITH, G. B. (2003). Optimization of a reusable

hollow-fiber ultrafilter for simultaneous concentration of enteric bacteria, protozoa, and viruses from water. *Appl. Environ. Microbiol.* **69**, (7), 4098-4102.
29. MOSCOVITS, M. (1985). Surface-enhanced spectroscopy. *Rev. Modern Phys.* **57**, (3), 783-826.
30. MOSIER-BOSS, P. A.; LIEBERMAN, S. H. (2003). Detection of volatile organic compounds using surface enhanced Raman spectroscopy substrates mounted on a thermoelectric cooler. *Anal. Chim. Acta* **488**, (1), 15-23.
31. MULLEN, K. I.; CRANE, L. G.; WANG, D. X.; CARRON, K. T. (1992). Trace detection of ionic species with surface enhanced raman spectroscopy. *Spectroscopy* **7**, (5), 24-32.
32. MUNIZ-MIRANDA, M.; INNOCENTI, M. (2004). AFM and micro-Raman investigation on filters coated with silver colloidal nanoparticles. *Appl. Surf. Sci.* **226**, (1-3), 125-130.
33. MURINDA, S. E.; NGUYEN, L. T.; IVEY, S. J.; GILLESPIE, B. E.; ALMEIDA, R. A.; DRAUGHON, F. A.; OLIVER, S. P. (2002). Molecular characterization of Salmonella spp. isolated from bulk tank milk and cull dairy cow fecal samples. *J. Food Prot.* **65**, (7), 1100-1105.
34. NAUJOK, R. R.; DUEVEL, R. V.; CORN, R. M. (1993). Fluorescence and Fourier-transform surface-enhanced Raman-scattering measurements of Methylene-Blue adsorbed onto a sulfur-modified gold electrode. *Langmuir* **9**, (7), 1771-1774.
35. PELLETIER, J. P. R.; TRANSUE, S.; SNYDER, E. L. (2006). Pathogen inactivation techniques. *Best Pract. Res. Clin. Haematol.* **19**, (1), 205-242.
36. QUINTERO-BETANCOURT, W.; PEELE, E. R.; ROSE, J. B. (2002). Cryptosporidium parvum and Cyclospora cayetanensis: a review of laboratory methods for detection of these waterborne parasites. *J. Microbiol. Methods* **49**, (3), 209-224.
37. SANCHEZ-CORTES, S.; DOMINGO, C.; GARCIA-RAMOS, J. V.; AZNAREZ, J. A. (2001). Surface-enhanced vibrational study (SEIR and SERS) of dithiocarbamate pesticides on gold films. *Langmuir* **17**, (4), 1157-1162.
38. SCHLICHTING, H. (1968). *Boundary Layer Theory*. New York:McGraw Hill.
39. SCHRODER, K.; MEYER-PLATH, A.; KELLER, D.; BESCH, W.; BABUCKE, G.; OHL, A. (2001). Plasma-induced surface functionalization of polymeric biomaterials in ammonia plasma. *Contrib. Plasma Phys.* **41**, (6), 562-572.
40. SOBSEY, M. D. (1999).Methods to identify and detect microbial contaminants in drinking water. In Press, National Academy, Ed. *Proceedings of the Strategies for Drinking Water Contaminants Conference*, Commission on Geosciences, Environment and Resources: Washington, DC; pp 173-205.
41. STRAUB, T. M.; CHANDLER, D. P. (2003). Towards a unified system for detecting waterborne pathogens. *J. Microbiol. Methods* **53**, (2), 185-197.
42. VO-DINH, T. (1995). SERS chemical sensors and biosensors: New tools for environmental and biological analysis. *Sens. Actuators, B* **29**, 183-189.
43. VO-DINH, T. (1998). Surface-enhanced Raman spectroscopy using metallic nanostructures. *Trends Anal. Chem.* **17**, (8-9), 557-582.
44. VOLKAN, M.; STOKES, D. L.; VO-DINH, T. (2005). A sol-gel derived AgCl photochromic coating on glass for SERS chemical sensor application. *Sens. Actuators, B - Chem.* **106**, (2), 660-667.

45. WALSH, R. J.; CHUMANOV, G. (2001). Silver coated porous alumina as a new substarte for surface-emhanced Raman scattering. *Appl. Spectr.* **55**, (12), 1695-1700.
46. WEISSENBACHER, N.; LENDL, B.; FRANK, J.; WANZENBOCK, H. D.; KELLNER, R. (1998). Surface enhanced Raman spectroscopy as a molecular specific detection system in aqueous flow-through systems. *Analyst* **123**, (5), 1057-1060.
47. WEISSENBACHER, N.; LENDL, B.; FRANK, J.; WANZENBOCK, H. D.; MIZAIKOFF, B.; KELLNER, R. (1997). Continuous surface enhanced Raman spectroscopy for the detection of trace organic pollutants in aqueous systems. *J. Mol. Struct.* **410**, 539-542.
48. WIESNER, M. R.; CHELLAM, S. (1999). The promise of membrane technologies. *Environ. Sci. Technol.* **33**, (17), 360.
49. WILKES, G. L.; LI, C. (1997). The mechanism for 3-Aminopropyltriethoxysilane to strengthen the interface of polycarbonate substrates with hybrid organic-inorganic sol-gel coatings. *J. Inorg. Organomet. Polym.* **7**, (4).

Figure Captions

Figure 1: Proposed mechanism for the APTMS reaction with polycarbonate and further silver chemisorption to the incorporated nitrogen

Figure 2: Micrographs of Ag nanoparticles: SEM image of filtered hydrosol (A), and TEM image of Ag nanoparticles deposited onto TEM grids by drop-coating (B). The size bar on the TEM micrograph corresponds to 20 nm.

Figure 3: Size distribution profile of silver nanoparticle suspension. Also shown are the predominant spherical diameters for the two major distribution peaks, and the estimated rod lengths for the two high end size peaks.

Figure 4: SEM micrographs of PCTE membrane filter that is non-modified (A), modified using APTMS linker (B, C, D), and modified using CysA linker (E, F). Images recorded at 13,000x (A, B, C, E), 40,000x (F), and 130,000x (D) magnifications.

Figure 5: UV-vis spectra of a modified PCTE membrane (bare membrane used as baseline), and of silver hydrosol (250 μL in 2 mL ultrapure water, ultrapure water used as baseline).

Figure 6: Absorption and Raman spectra of methylene blue.

Figure 7: Raman spectra of an untreated membrane (bottom) and modified membrane (top).

Figure 8: Raman spectrum of a 1 mmol/L aqueous solution of MB (bottom), a 10^{-5} mol/L aqueous solution of MB in pre-coagulated silver sol (middle), and a 10^{-5} mol/L aqueous solution of methylene blue after “drop and dry” on a modified membrane.

Figure 9: Box plots for enhancement factors of MB on precoagulated sol and modified membranes (A) and after preconcentration of modified membranes (B).

Figure 10: Results of clean water flux test for bare and modified membranes.

Figure 11: Raman spectrum of a 10^{-7} mol/L aqueous solution of MB after 2 hours of pre-concentration on a modified membrane.

Figures

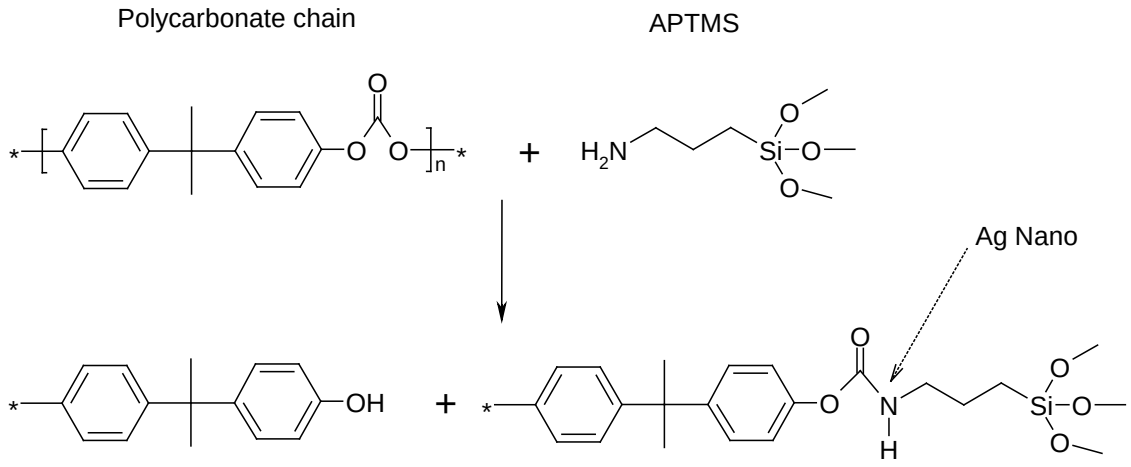

Figure 1: Proposed mechanism for the APTMS reaction with polycarbonate and further silver chemisorption to the incorporated nitrogen

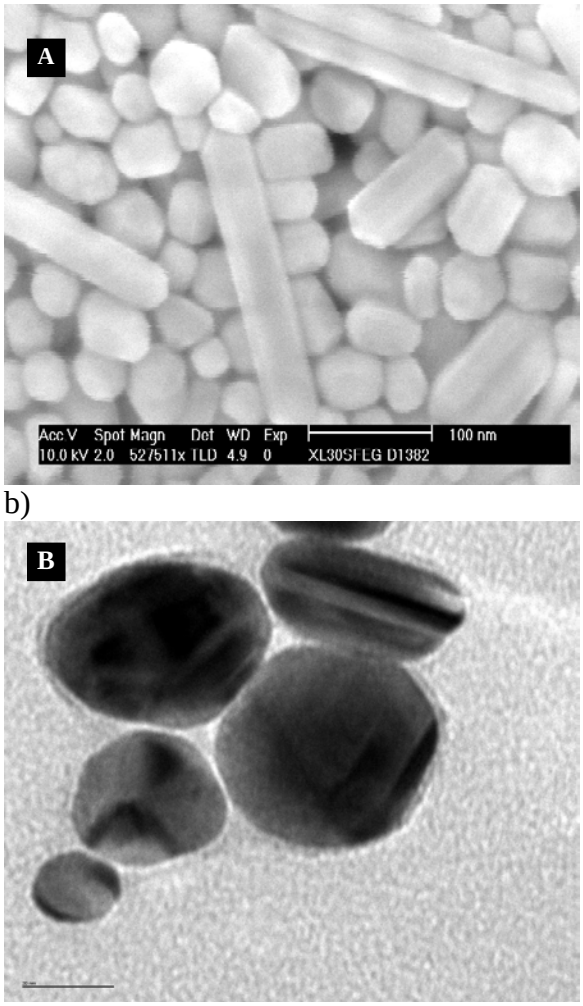

Figure 2: Micrographs of Ag nanoparticles: SEM image of filtered hydrosol (A), and TEM image of Ag nanoparticles deposited onto TEM grids by drop-coating (B). The size bar on the TEM micrograph corresponds to 20 nm.

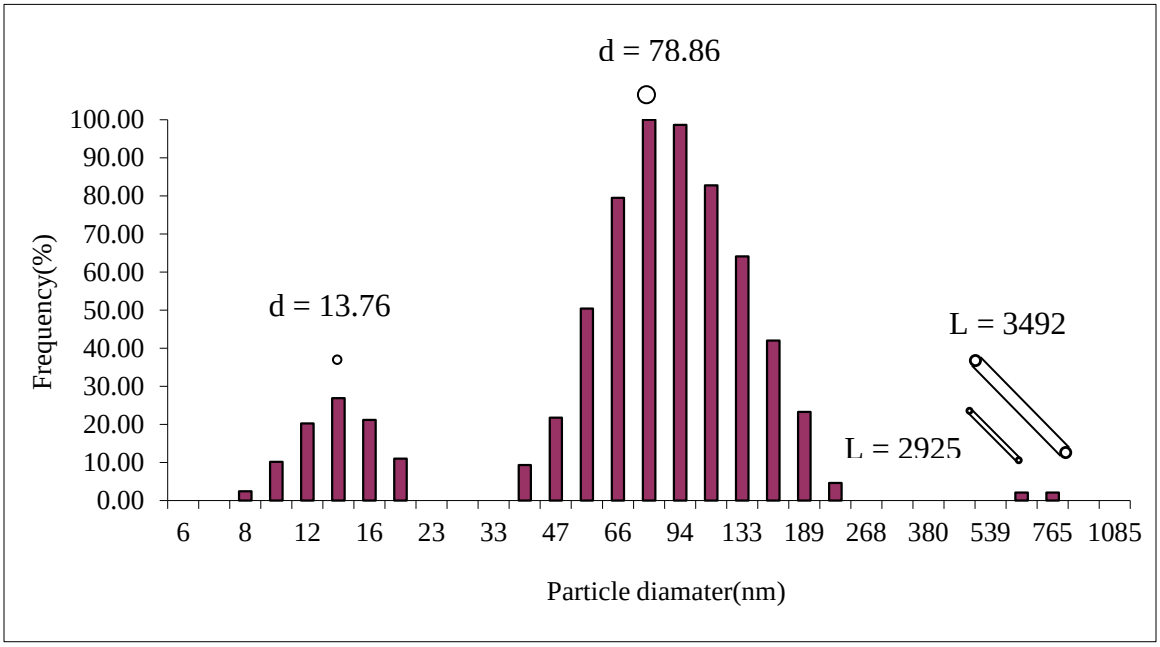

Figure 3: Size distribution profile of silver nanoparticle suspension. Also shown are the predominant spherical diameters for the two major distribution peaks, and the estimated rod lengths for the two high end size peaks.

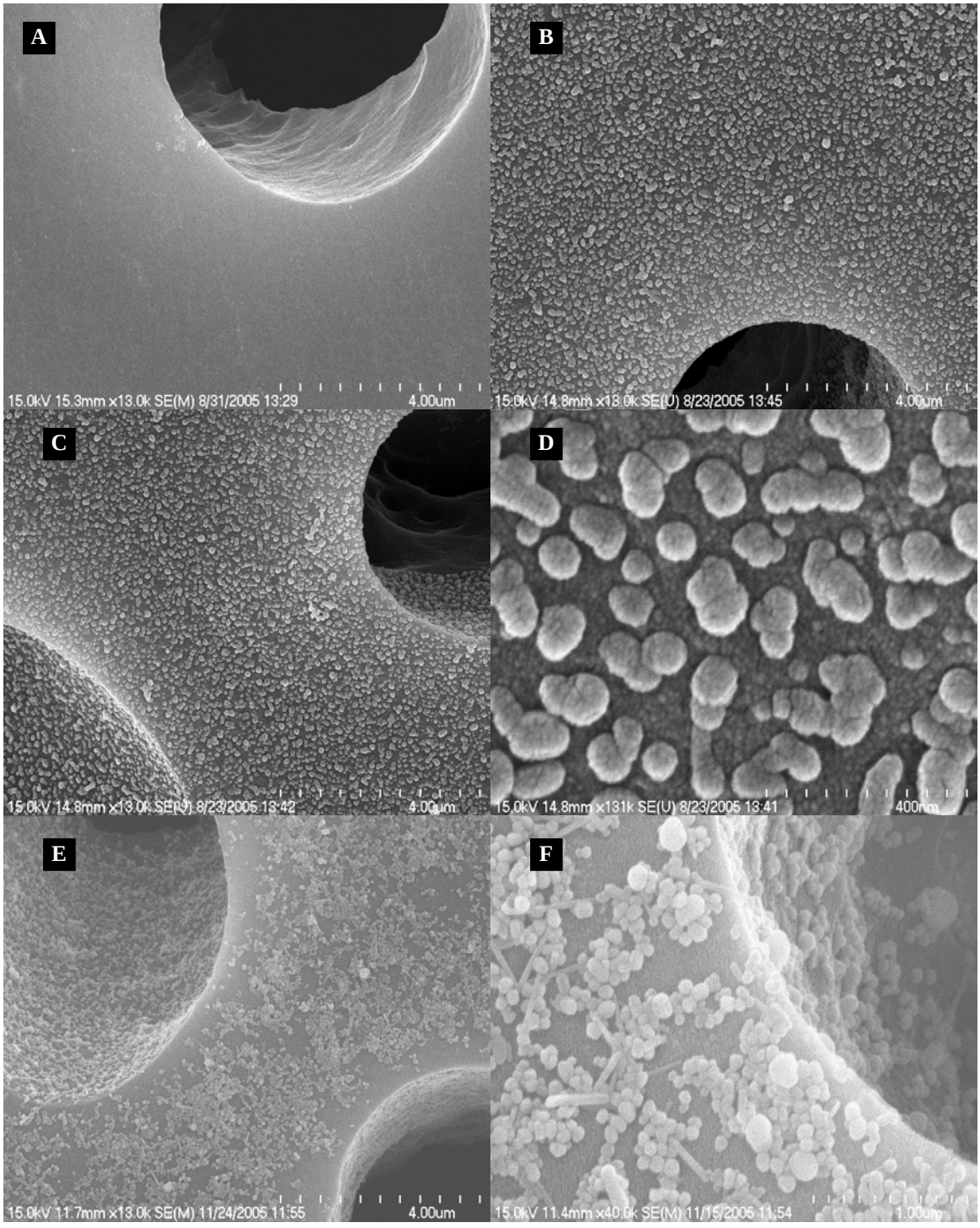

Figure 4: SEM micrographs of PCTE membrane filter that is non-modified (A), modified using APTMS linker (B, C, D), and modified using CysA linker (E, F). Images recorded at 13,000x (A, B, C, E), 40,000x (F), and 130,000x (D) magnifications.

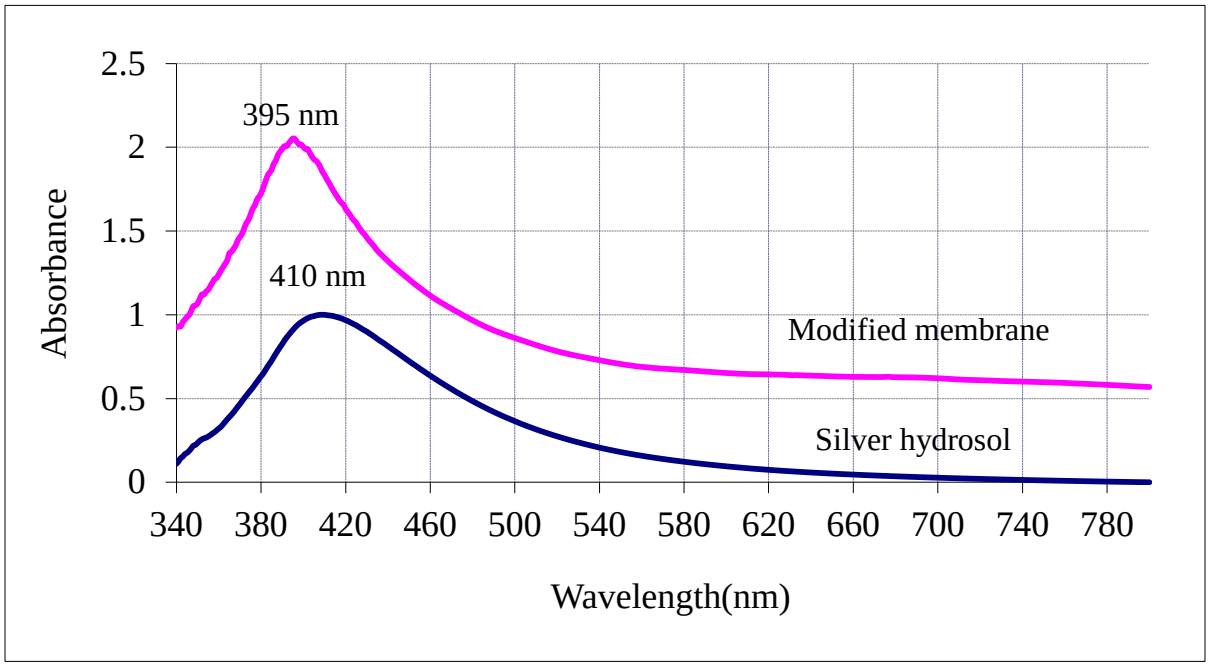

Figure 5: UV-vis spectra of a modified PCTE membrane (bare membrane used as baseline), and of silver hydrosol (250 μL in 2 mL ultrapure water, ultrapure water used as baseline).

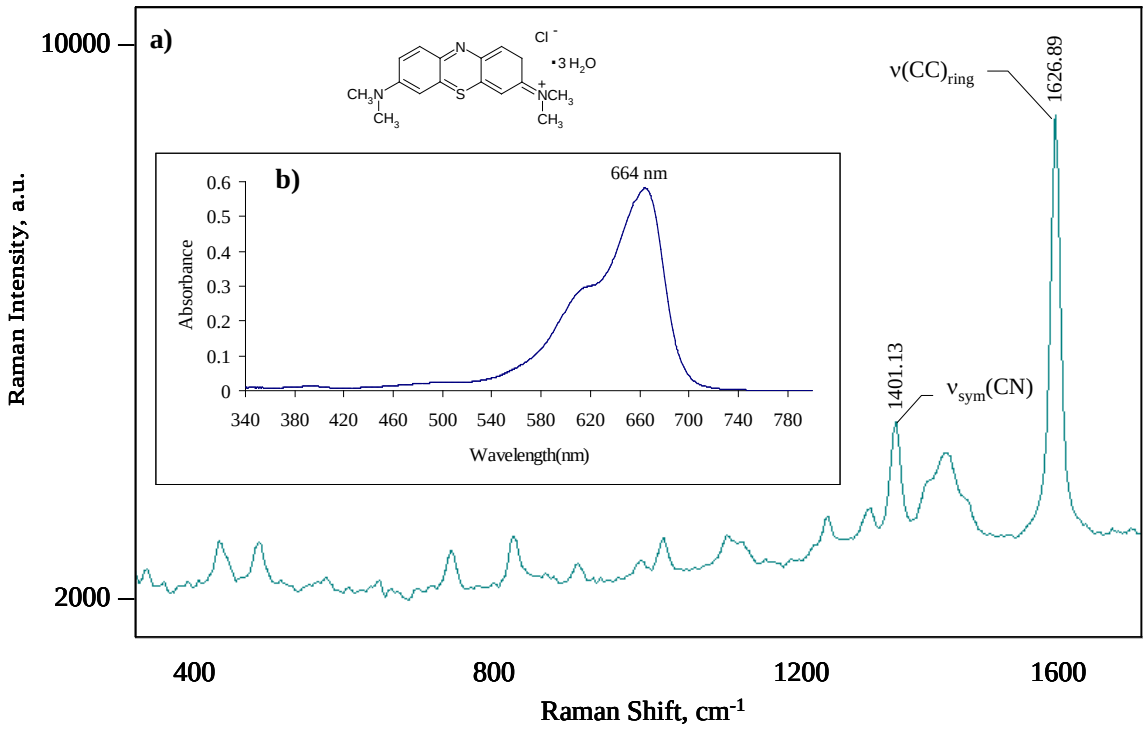

Figure 6: Absorption and Raman spectra of methylene blue.

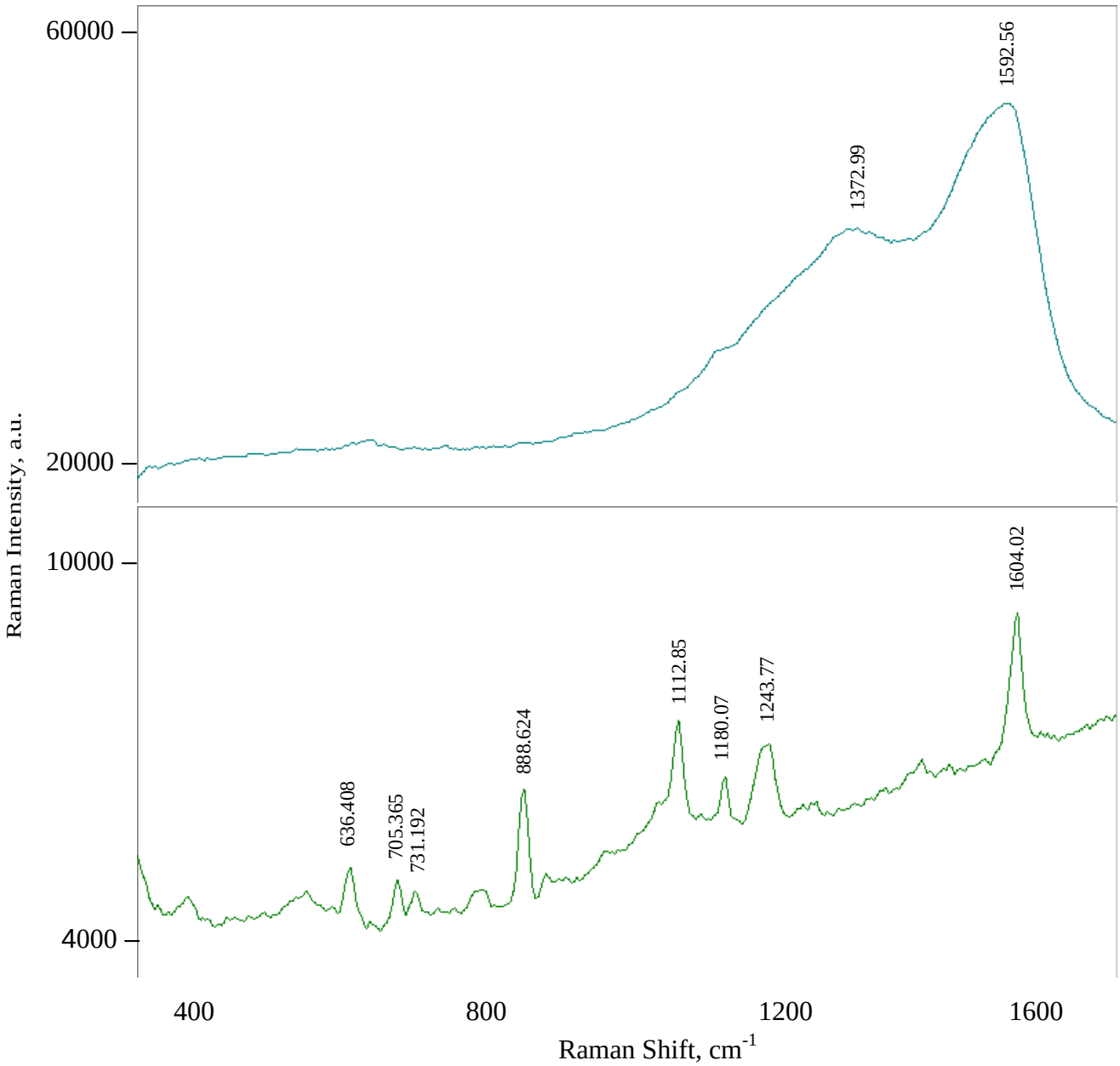

Figure 7: Raman spectra of an untreated membrane (bottom) and modified membrane (top).

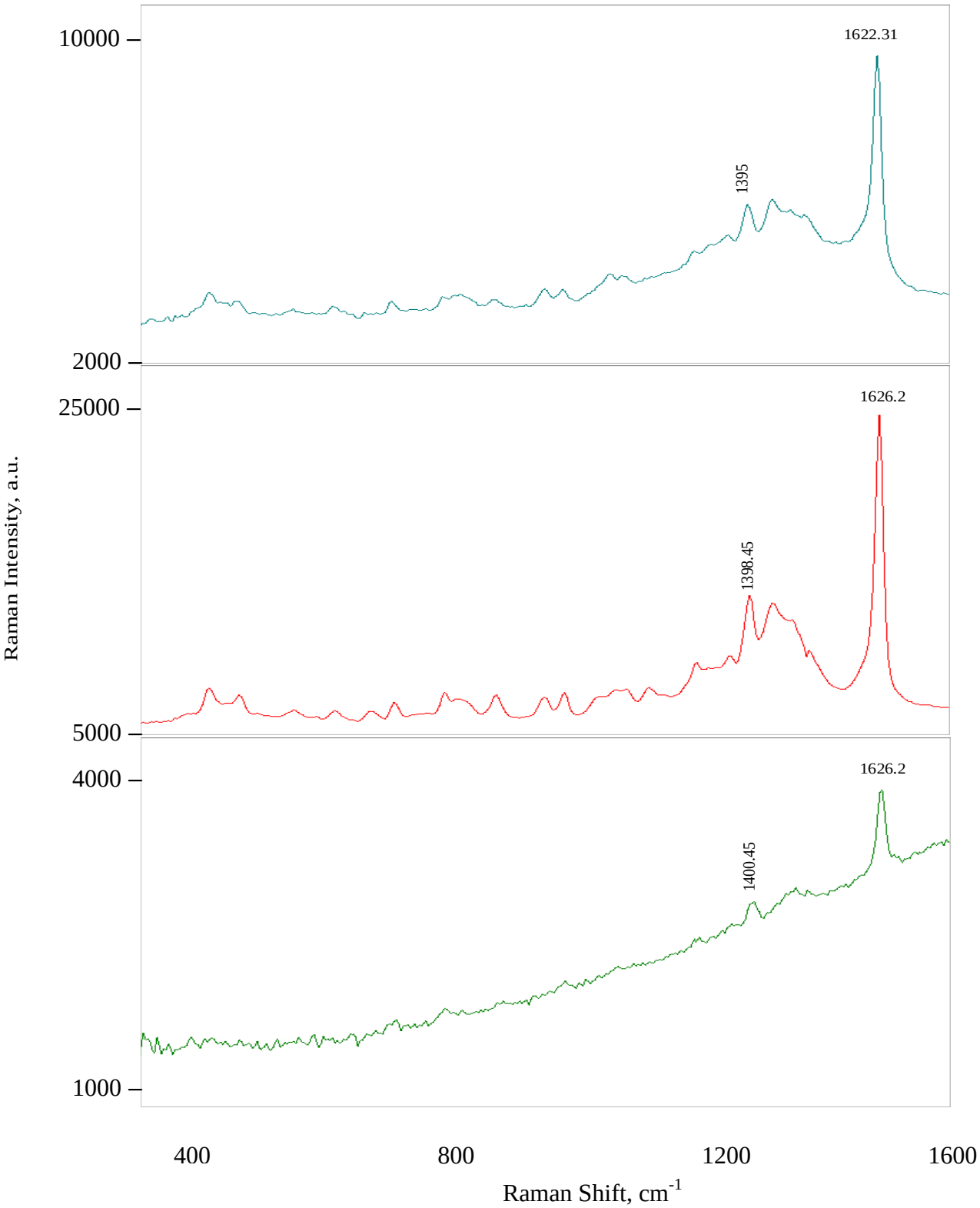

Figure 8: Raman spectrum of a 1 mmol/L aqueous solution of methylene blue (bottom), a 10^{-5} mol/L aqueous solution of MB in pre-coagulated silver sol (middle), and a 10^{-5} mol/L aqueous solution of methylene blue after “drop and dry” on a modified membrane

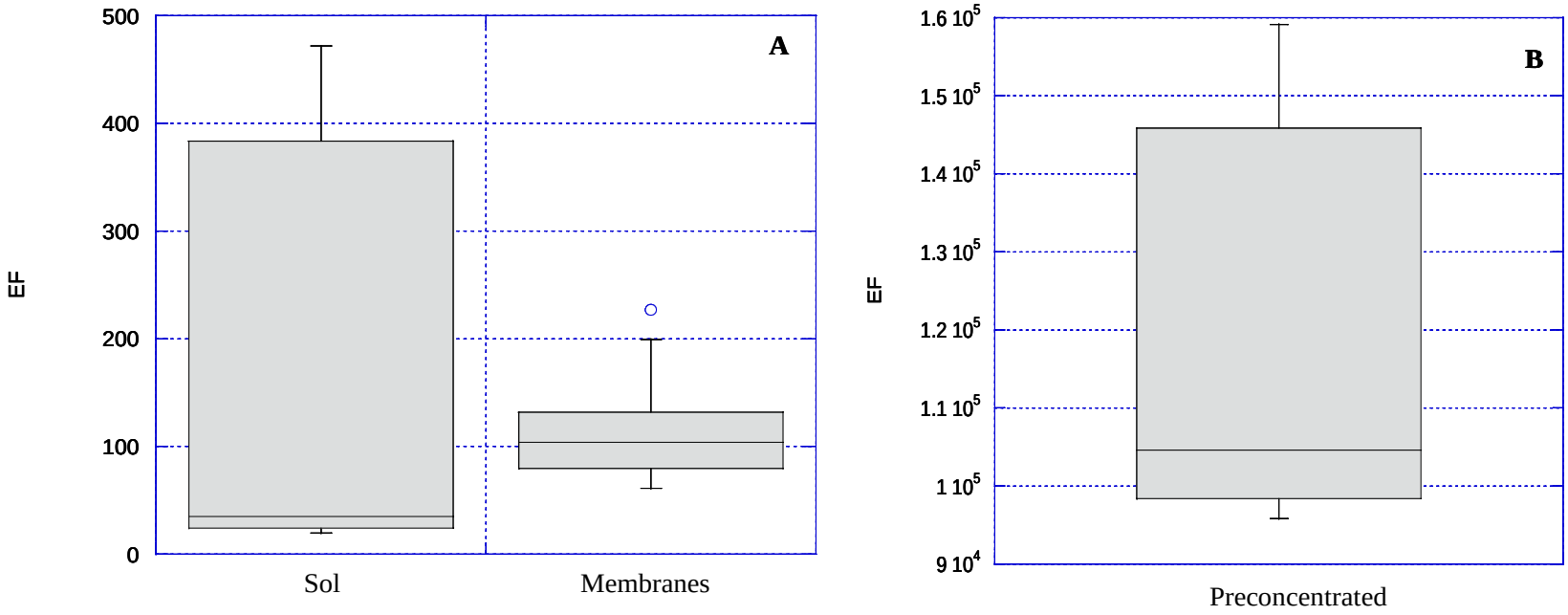

Figure 9: Box plots for enhancement factors of MB on precoagulated sol and modified membranes (A) and after preconcentration using modified membranes (B).

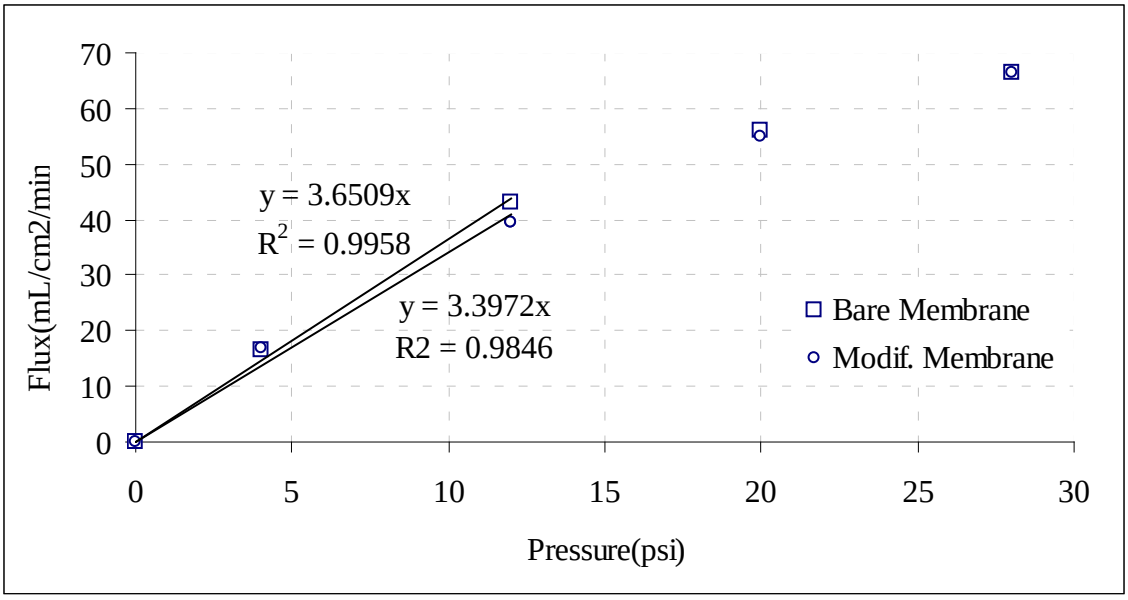

Figure 10: Results of clean water flux test for bare and modified membranes.

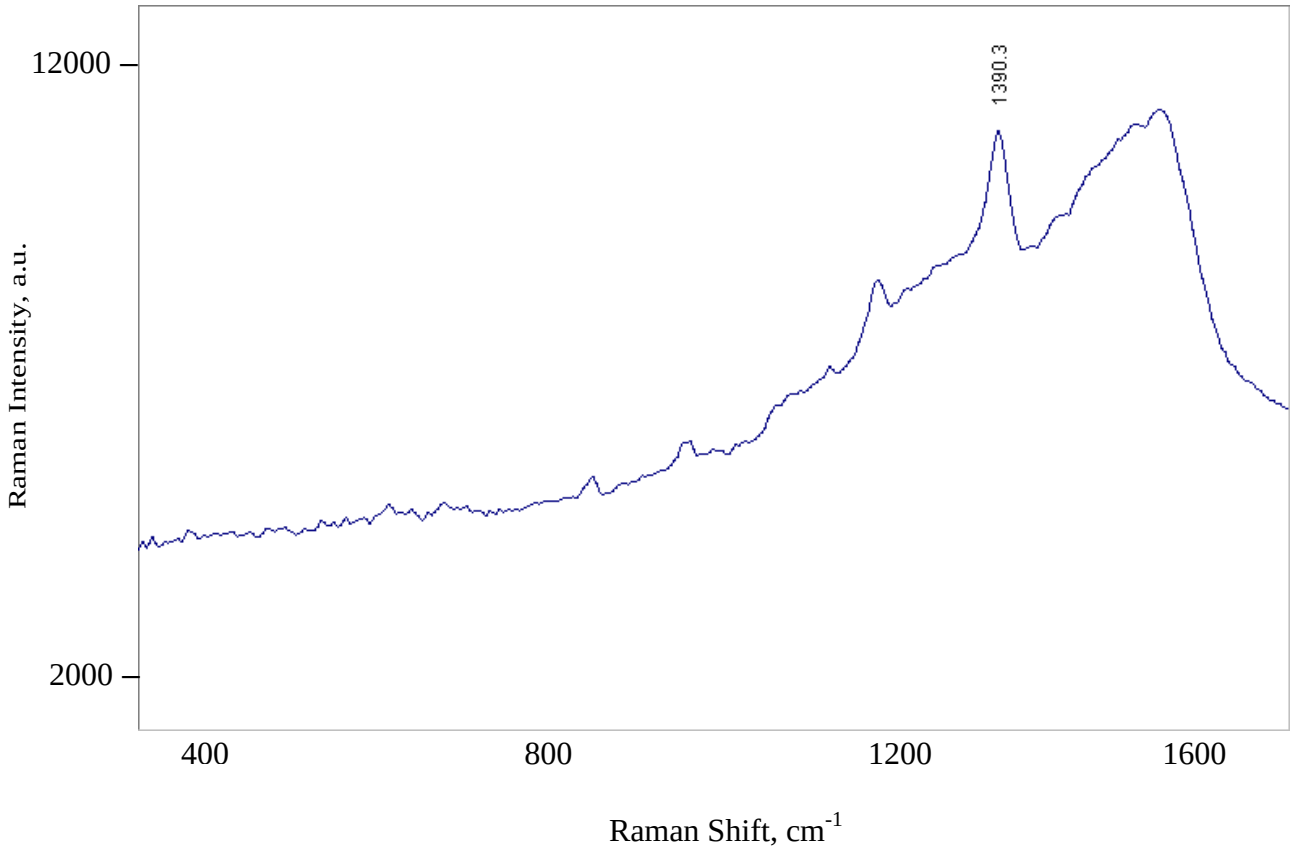

Figure 11: Raman spectrum of a 10^{-7} mol/L aqueous solution of MB after 2 hours of pre-concentration on a modified membrane.